Groundwater

Physically Based Groundwater Vulnerability Assessment Using Sensitivity Analysis Methods

by Jean Beaujean[1,2], Jean-Michel Lemieux[1,3], Alain Dassargues[1], René Therrien[4], and Serge Brouyère[5]

Abstract

A general physically based method is presented to assess the vulnerability of groundwater to external pressures by numerical simulation of groundwater flow. The concept of groundwater vulnerability assessment considered here is based on the calculation of sensitivity coefficients for a user-defined groundwater state for which we propose several physically based indicators. Two sensitivity analysis methods are presented: the sensitivity equation method and the adjoint operator method. We show how careful selection of a method can significantly minimize the computational effort. An illustration of the general methodology is presented for the Herten aquifer analog (Germany). This application to a simple, yet insightful, case demonstrates the potential use of this general and physically based vulnerability assessment method to complex aquifers.

Introduction

Vulnerability assessment studies are becoming increasingly popular to assist land-use planning and related decisions about groundwater protection. Maps that show groundwater vulnerability to potential threats located at ground surface are the most accepted tools because they are simple, visually attractive, and can be used in geographical information systems (GIS) for decision support.

The most popular methods to assess groundwater vulnerability are index-based (Gogu and Dassargues 2000). These methods, such as DRASTIC (Aller et al. 1987), EPIK (Doerfliger et al. 1999), and GOD (Foster 1987), represent with physical attributes, the protective effects of layers overlying an aquifer. These attributes are then weighted to generate a vulnerability index from which a gridded vulnerability map can be generated. The resulting vulnerability index strongly depends on the values chosen for the physical attributes along with the associated weight embedded in the assessment methods. As mentioned by Neukum et al. (2008), the main advantages of index-based weights approaches for practical applications are their simplicity and limited data requirement. However, comparison of existing index-based methods shows that they can provide contradictory results for a given case study (Gogu et al. 2003). Physically based methods that rely on numerical simulation of groundwater flow and solute transport have recently been proposed to resolve those contradictions associated with index-based methods (e.g., Brouyère et al. 2001; Frind et al. 2006; Popescu et al. 2008; Neukum et al. 2008; Molson and Frind 2012).

While most groundwater vulnerability assessment methods and studies have focused on contamination issues, it is now recognized that there are several other stress factors that are likely to threaten groundwater systems such as predicted changes in precipitation and groundwater recharge. In this context, a more general methodology, which also relies on a physically based concept, is needed for evaluating and quantifying the potential impact of stress factors on both groundwater quantity and quality.

The European Community has recently put forward the DPSIR framework, which describes the interactions between society and the environment (EEA 2003). The DPSIR framework defines a chain of Drivers that exert Pressures on the State of a given resource, such as water, which then generates an Impact that will require an appropriate Response (Kristensen 2004). This framework

[1]Hydrogeology & Environmental Geology, Geo3 Group, ArGEnCo Department, Aquapôle, B-52/3, Université de Liège, B-4000 Liège, Belgium.

[2]Currently at Applied Geophysics, Geo3 Group, ArGEnCo Department, Université de Liège, Liège, Belgium.

[3]Currently at Département de Géologie et de Génie Géologique, Université Laval, 1065 Avenue de la Médecine, Québec, Canada.

[4]Département de Géologie et de Génie Géologique, Université Laval, 1065 avenue de la Médecine, Québec, Canada.

[5]Corresponding author: Hydrogeology & Environmental Geology, Geo3 Group, ArGEnCo Department, Aquapôle, B-52/3, Université de Liège, B-4000 Liège, Belgium; +32-436-62377; fax: +32-436-69520; serge.brouyere@ulg.ac.be

Received June 2012, accepted September 2013.

doi: 10.1111/gwat.12132

is general and, when applied to water, can include states that are not limited to quality such as, for example, water quantity and availability.

In this paper, we present a general physically based method to assess the vulnerability of groundwater to external pressures. The method combines numerical groundwater flow and the DPSIR framework. The concept of groundwater vulnerability assessment is based on sensitivity coefficients that reflect the easiness with which the groundwater state transmits pressures into impacts. These coefficients are grouped into a vulnerability matrix of pressures and impacts that quantify vulnerability for every combination of causal links identified in the DPSIR chain. The sensitivity coefficients are converted to vulnerability using the concept of falling below a given threshold, which is commonly used in socioeconomic sciences (Luers et al. 2003). To define and evaluate the sensitivity coefficients, several physically based indicators are proposed for the groundwater state as affected by different types of pressures (Gardin et al. 2006; Beaujean et al. 2008).

Sensitivity analysis methods have been traditionally used for automatic calibration or inverse modeling (e.g., Sun and Yeh 1990), for uncertainty analysis (Jyrkama and Sykes 2006), for optimization (e.g., Ahlfeld et al. 1988), and to assess the sensitivity of a model to its parameters and boundary conditions (Sykes et al. 1985). Sensitivity analysis methods are used here for a different purpose, which is to evaluate the vulnerability of the state of the system to local variations in external pressures under the assumption that a groundwater flow model has already been calibrated. The sensitivity analysis method is therefore used here as a tool for decision making and aquifer management support. This paper emphasizes that the choice of a sensitivity analysis method with respect to the management objectives should generate insightful vulnerability coefficients while minimizing the computational effort. Two sensitivity analysis methods are considered in the context of groundwater vulnerability assessment: the sensitivity equation method and the adjoint operator method.

An illustration of the general methodology is presented for a synthetic alluvial aquifer with concerns related to water supply. This application of sensitivity analysis to a simple, yet insightful, case demonstrates the potential of this general and physically based vulnerability assessment method for application to complex aquifers.

Underlying Concepts

DPSIR Framework

The DPSIR framework describes the interactions between society and the environment based on the assumption that there is a causal chain between social and economic developments linked to anthropogenic activities, such as agriculture and industry (*drivers*), and *pressures* exerted on the *state* of the environment, such as excessive use of resources, changes in land use and air emissions, water, and soil. The state of the environment is the combination of the physical, chemical, and biological conditions that are modified and degraded by the pressures. The *impacts* are the consequences of those changes in the physical, chemical, and biological conditions (*states*) of the environment, which modify the behavior of ecosystems, their life-supporting abilities, and ultimately human health and socioeconomic performance of the society. These undesired impacts require *responses* from society to improve the state of the environment. Responses can affect any part of the causal chain.

To develop a conceptual model that combines the DPSIR approach with a systematic and physically based representation of the groundwater system, it is proposed here to further describe the *state* component (ST) of the DPSIR chain by identifying explicitly : (1) "state upstream factors" (UFs), which are the physical elements or factors that relate state variables to pressures and (2) the "state downstream factors" (DFs), which are the physical elements or factors that relate state variables to impacts. Examples of state UFs are groundwater recharge or well abstraction, and examples of state DFs are reduction in base flow or changes in groundwater levels.

Quantitative Description of Groundwater Vulnerability

Groundwater state vulnerability can be defined as a series of sensitivity coefficients, S, that relate impacts I to pressures P:

$$S \equiv S_{ij} = \frac{\partial I_j}{\partial P_i} \qquad i = 1, n_{\mathrm{P}}; \quad j = 1, n_{\mathrm{I}} \qquad (1)$$

where n_{I} and n_{P} are the number of impacts and pressures considered, respectively.

Using the definition of UFs and DFs provided earlier, sensitivity coefficients define how a change in a given UF has direct effects on DFs or groundwater ST. One example would be the impact of changes in groundwater recharge (UF) on baseflow (DF) or water table elevation (ST). This refinement within STs of the DPSIR chain distinguishes between groundwater resource vulnerability (GRV) and groundwater source vulnerability (GSV) (Brouyère et al. 2001). GRV reflects the vulnerability of an entire aquifer to a given pressure, for example contamination, while GSV is the vulnerability of specific components of the groundwater system, for example, a pumping well. Using this methodology, we can extend the groundwater vulnerability concept to stresses other than contamination. For example, the vulnerability of a pumping well to changes in groundwater recharge could be evaluated. Sensitivity coefficients can then be further defined independently for groundwater source S_{ij}^{GS} and resource S_{ij}^{GR}:

$$S_{ij}^{\mathrm{GS}} = \frac{\partial DF_j}{\partial UF_i} \qquad i = 1, n_{\mathrm{P}}; \quad j = 1, n_{\mathrm{I}} \qquad (2)$$

$$S_{ij}^{\mathrm{GR}} = \frac{\partial ST_j}{\partial UF_i} \qquad i = 1, n_{\mathrm{P}}; \quad j = 1, n_{\mathrm{I}}. \qquad (3)$$

The definition of groundwater vulnerability using sensitivity coefficients emphasizes the sensitivity of the groundwater resource/source to pressures but it does not indicate how far the current state of the groundwater resource/source is from a critical damaged state. To resolve this problem, Luers et al. (2003) extended the concept of sensitivity as defined above to the definition of system vulnerability, V, by defining a ratio that reflects the "distance" between the current state of the water system and its "damaged state":

$$V = \text{sensitivity}/\text{state relative to threshold} \tag{4}$$

$$= \frac{|S_{ij}|}{W/W_0} \tag{5}$$

where W is the current state and W_0 is the threshold above which the system is assumed to be damaged.

In this study, the vulnerability coefficient is normalized by the maximum calculated sensitivity coefficient:

$$V' = \frac{V}{S_{\max}}. \tag{6}$$

Therefore, a value of 1 means that the groundwater system is damaged and its sensitivity is the largest. A lower value indicates that the groundwater system (source or resource) is either damaged or its current state is being degraded but its sensitivity is less than or equal to the maximum sensitivity. For example, for two equally sensitive scenarios, the one for which the current state is closer to the threshold will represent a more vulnerable scenario. The separate use of the ratio W/W_0 or sensitivity coefficients alone are therefore not sufficient to define vulnerability and a choice of a threshold must be made. The latter is an end-user choice and consists of maximal/minimal acceptable values of well-being, such as the lowest acceptable groundwater level associated with maintaining a safe yield to protect groundwater resource.

Sensitivity Analysis

There are three main methods to compute the sensitivity coefficients that can be grouped into two general categories. The first category is a differential approach, which relies on the derivative of the performance measure with respect to the system parameter/boundary conditions. The derivative can be computed with a perturbation method or the sensitivity equation method, which uses the derivative as a primary variable. In this paper, we only use the sensitivity equation method because it is more accurate. The second category is a variational approach also known as the adjoint operator method. These methods are presented in details in the Supporting Information along with the fluid continuity equation and its numerical discretization with the Galerkin finite-element method.

The sensitivity equation method is most appropriate for assessing the GRV because it enables the calculation of spatially distributed sensitivity coefficients to a local change in boundary conditions/parameters. For example, the sensitivity equation method would be appropriate to assess the sensitivity of hydraulic heads in an aquifer to a change in the abstraction rate at a pumping well. The adjoint operator method is most appropriate for GSV because the solution is the sensitivity of a selected (and often local) performance measure, to a spatially distributed set of changes in the boundary conditions/parameters. For instance, it could be used to obtain the sensitivity of the hydraulic head in an observation well to a change in pumping rate at multiple pumping wells in the aquifer.

These concepts are illustrated for the theoretical aquifer as shown in Figure 1a, where the hydraulic head field is given by $h(\mathbf{x})$ and where there are n_w pumping wells and one observation well located at x_p ($\mathbf{x}$ denotes a continuous field while x_p denotes a point location). The differential approach is illustrated in Figure 1b, where the sensitivity of the resource (e.g., hydraulic heads in the entire aquifer) to a change dQ_2 in pumping rate

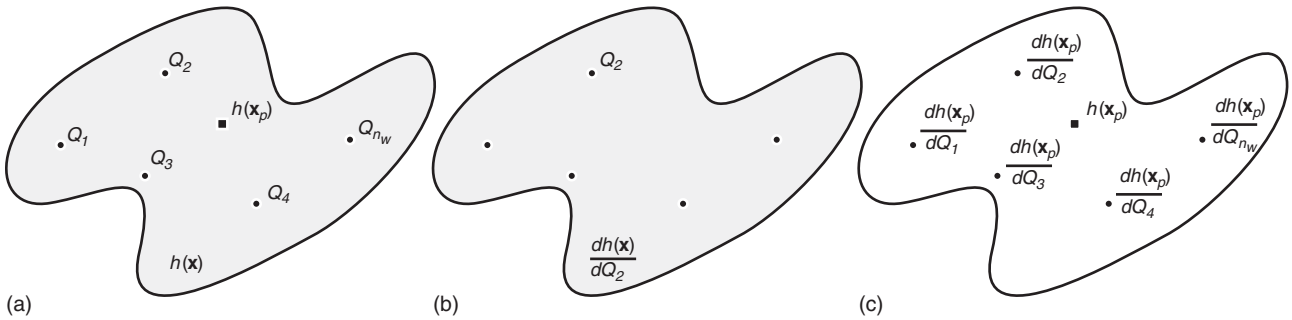

Figure 1. Illustration of the two main approaches to calculate the sensitivity coefficients. (a) Theoretical aquifer with hydraulic heads given by $h(x)$ in which there are n_w pumping wells and an observation point $h(x_p)$. The aquifer is shaded to indicate that the hydraulic head is a continuous variable. (b) Differential approach where the sensitivity of the aquifer water levels $dh(x)/dQ_2$ are given with respect to a change in pumping rate at well Q_2 (resource sensitivity). The aquifer is shaded to indicate that the sensitivity coefficients are continuous over the aquifer. (c) Adjoint operator approach where the sensitivity of the water level $dh(x_p)/dQ_i$ at point $h(x_p)$ is calculated with respect to a change in every pumping well Q_i (source sensitivity). The aquifer is not shaded because the sensitivity coefficients are not continuous over the aquifer, but calculated at discrete points.

at pumping well 2 is given by $S(\mathbf{x})_2 = \mathrm{d}h(\mathbf{x})/\mathrm{d}Q_2$. The result is a spatial and continuous distribution of sensitivity coefficients illustrated by the shaded area in Figure 1b. The general solution of the differential approach is a sensitivity field $S(\mathbf{x})$ with respect to any pumping well, which is given by

$$S(\mathbf{x})_i = \frac{\mathrm{d}h(\mathbf{x})}{\mathrm{d}Q_i} \qquad \text{for } i = 1, n_\mathrm{w} \tag{7}$$

which means that there is a different sensitivity field for every pumping well.

The adjoint operator method is shown in Figure 1c where it is used to infer source sensitivity. In this approach, the sensitivity of the hydraulic heads $h(x_\mathrm{p})$ at the observation point location x_p with respect to a change $\mathrm{d}Q_i$ in pumping rate at well i is given by

$$S(x_\mathrm{p})_i = \frac{\mathrm{d}h(x_\mathrm{p})}{\mathrm{d}Q_i} \qquad \text{for } i = 1, n_\mathrm{w}. \tag{8}$$

In this case, the solution is a sensitivity coefficient for each discrete location i. Here, there are five pumping wells such that there are five point sensitivity coefficients shown in Figure 1c.

The sensitivity coefficients can be computed for any user-defined parameters. To this end, we define $\{\alpha\}$ as an array of model parameters used for the sensitivity analysis:

$$\begin{aligned}\{\alpha\} &= \{\alpha_1, \alpha_m, \ldots, \alpha_M\} \\ &= \left\{K_{ij}(\mathbf{x}), S_s(\mathbf{x}), Q(\mathbf{x}), h_0(\mathbf{x}), \widehat{h}(\mathbf{x}), \widehat{q}(\mathbf{x}), \ldots\right\}\end{aligned} \tag{9}$$

where α_m is the mth parameter of the array and M is the total number of parameters. The model parameters can include both the boundary conditions as well as physical properties (e.g., K_{ij}, S_s). The model parameters are used to link external pressures to UFs. For instance, climate change is a pressure that can yield a change in groundwater recharge (the UF) which is represented in the model by a specified flux boundary condition. Conceptually, all model parameters can be linked to pressures. Another example is the change in hydraulic conductivity that can result from the dissolution of minerals owing to a change in water chemistry.

The array of parameters $\{\alpha\}$ can also be a single spatially distributed physical property such as

$$\{\alpha\} = \{\widehat{q}_i\} \quad \text{for } i = 1, n_q \tag{10}$$

where n_q is the number of specified flux boundaries in the model. In this case, the total number of parameters would be $M = n_q$.

The sensitivity equation and the adjoint operator methods require code modifications if an existing groundwater flow model is used (see Supporting Information for details). On the other hand the modifications are very minor because the sensitivity and adjoint equations have the same form as the fluid continuity equation.

The choice of a sensitivity analysis method is solely made to reduce the computational effort, because the three methods will provide the same results. It can be shown that for each type of problem, there is one sensitivity analysis method that can significantly reduce the number of simulations required to compute the sensitivity coefficients. Consider the problem discussed in the previous section and assume that the domain is discretized with n_n nodes. We could use all three methods to compute resource sensitivity $\mathrm{d}h(\mathbf{x})/\mathrm{d}Q_i$. If we assume that the number of parameters is $M = n_\mathrm{w}$ and the number of performance measures is $L = n_\mathrm{n}$ (i.e., the number of nodes in the model), we would need $n_\mathrm{w} + 1$ (i.e. $M + 1$) simulations with the sensitivity equation methods but $n_\mathrm{n} + 1$ (i.e., $L + 1$) simulations with the adjoint operator method. Because the number of nodes n_n is generally much larger than the number of performance measures n_w for a typical groundwater flow simulation, the sensitivity equation method is much more efficient.

We can also look at source sensitivity $\mathrm{d}h(x_\mathrm{p})/\mathrm{d}Q_i$. With the perturbation method, the number of simulations required is $n_\mathrm{w} + 1$ (i.e., $M + 1$). On the other hand, the number of performance measures is $L = 1$, so the number of simulations with the adjoint operator method would be 2 (i.e., $L + 1$). The adjoint method is therefore more efficient when $L < M$.

Demonstration

This method is illustrated using the geostatistical reconstruction of the Herten high-resolution fluvio-glacial aquifer analog (Comunian et al. 2011) from Germany. The reconstruction is based on six high-resolution parallel vertical profiles, each having a size of 16 m × 10 m, that were mapped with a resolution of 5 cm with respect to structural and hydraulic properties (Bayer et al. 2011). The original analog model has over 9 million cubic elements but was downscaled to 1,119,000 elements to reduce the computational effort. For downscaling, each element of the coarser model was mapped on the finer model and the dominant facies was assigned to the downscaled, coarser model. When no dominant facies could be identified, the facies for the coarser model was randomly selected. Figure 2 shows the distribution of the hydro-facies and corresponding hydraulic conductivity, while Table 1 provides a description of the facies. The dimensions of the analog aquifer were multiplied by a factor of 10 for the groundwater flow simulations to provide a more realistic aquifer size. The resulting dimensions are 160 m × 100 m × 70 m for the simulated aquifers. In addition, the hydraulic conductivity of the cGcg facies, which is dominant in the upper part of the aquifer, was increased by one order of magnitude.

The control-volume finite-element model HydroGeoSphere (Therrien et al. 2006) is used for the demonstration. It was modified to include the adjoint operator method as well as the sensitivity equation method

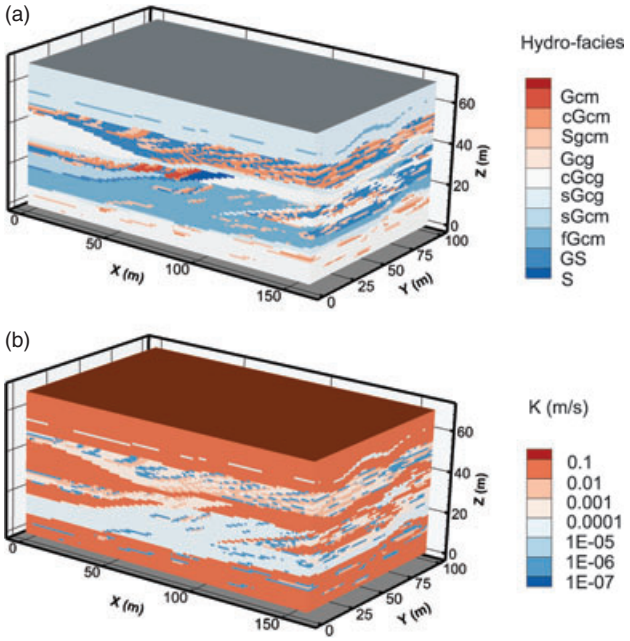

Figure 2. (a) Downscaled reconstruction of the Herten aquifer analog showing the distribution of hydro-facies. See Table 1 for description of units. (b) Hydraulic conductivity distribution.

following the development shown in the Supporting Information.

The simulation domain of the coarser model is discretized with uniform cubic elements having dimensions of 1 m × 1 m × 1 m. Fully saturated steady-state flow is simulated. A head value of 65 m is prescribed at $x = 160$ m and a recharge rate of 300 mm/year is prescribed on the entire surface of the model. The other limits of the model are no-flow boundaries. In this study, we considered two models. In the first model (Model 1), a shallow pumping well is tapping the sGcg hydro-facies. The bottom is located at coordinates $x = 75$ m, $y = 75$ m, and $z = 60$ m and is screened over 3 m (shown as a black square in Figure 3a). A low withdrawal rate is set to 2 m^3/d. In a second model (Model 2), a deep pumping well is tapping the cGcg hydro-facies located at coordinates $x = 75$ m, $y = 75$ m, and $z = 44$ m and is screened over 3 m (shown as a black square in Figure 3b). The latter is characterized by the same low pumping rate. The simulated hydraulic heads are shown in Figure 3a and 3b (left). Because the upper part of the aquifer has a very large hydraulic conductivity, the horizontal gradient in the upper layer is very weak. On the other hand, because of many low hydraulic conductivity layers, the vertical gradient is much stronger. Figure 3a and 3b (right) are two cross sections located at coordinate $y = 75$ m that show the direction of groundwater flow within the aquifer along with the distribution of hydraulic conductivity. It shows that groundwater flow is focused in a few permeable layers.

Table 1
Hydro-Facies Description and Hydraulic Conductivity

Hydro-Facies	Description	K (m/s)
Gcm	Poorly sorted, matrix supported gravel, Normal	2.5×10^{-4}
cGcm	Poorly sorted, matrix supported gravel, Cobble-rich	2.3×10^{-4}
sGcm	Sand-rich	6.1×10^{-5}
Gcg, o	Alternating gravel, matrix-free, clast-supported open framework coarse-fine pebbles	2.6×10^{-2}
cGcg, o	Alternating gravel, cobbles-coarse pebbles openwork	1.3×10^{-2}
sGcg, o	Alternating gravel, granules/sand open framework	9.5×10^{-2}
sGcm, b	Alternating gravel, bimodal basal subunit with sand matrix	4.3×10^{-5}
fGcm, b	Alternating gravel, bimodal basal subunit with silt/clay matrix	6.0×10^{-7}
GS-x	Well sorted gravel (and coarse sand)	2.3×10^{-3}
S-x	Pure, well sorted sand	1.4×10^{-4}

Modified from Bayer et al. (2011).

Source Vulnerability

As a first demonstration, GSV is assessed using the adjoint operator method. One scenario is considered for the two models. In this scenario, climate change is the pressure and the UF is groundwater recharge (Table 2). The DF is hydraulic head and the performance measure is the hydraulic head at a pumping/observation well. The impact is the reduction in water availability or groundwater depletion.

The shallow and deep observation wells mentioned previously are considered, such that there are two sensitivity coefficients. Figure 4a and 4b shows the simulated sensitivity coefficients of the groundwater head in the wells with respect to an elemental surface change in groundwater recharge. Sensitivity coefficients provide information on the areas where a change in groundwater recharge is most likely to have an impact on hydraulic heads at the observation wells. These values are only available for the ground surface where the recharge was prescribed. Inspection of the sensitivity coefficients in Figure 4a shows that the most sensitive areas are directly above the shallow observation well. However, Figure 4b shows that the most sensitive areas are not necessarily above the deep observation well but are located upgradient. Sensitivity is higher in that area because hydraulic conductivity layers located above the observation well are pinching or thinning in that part of the

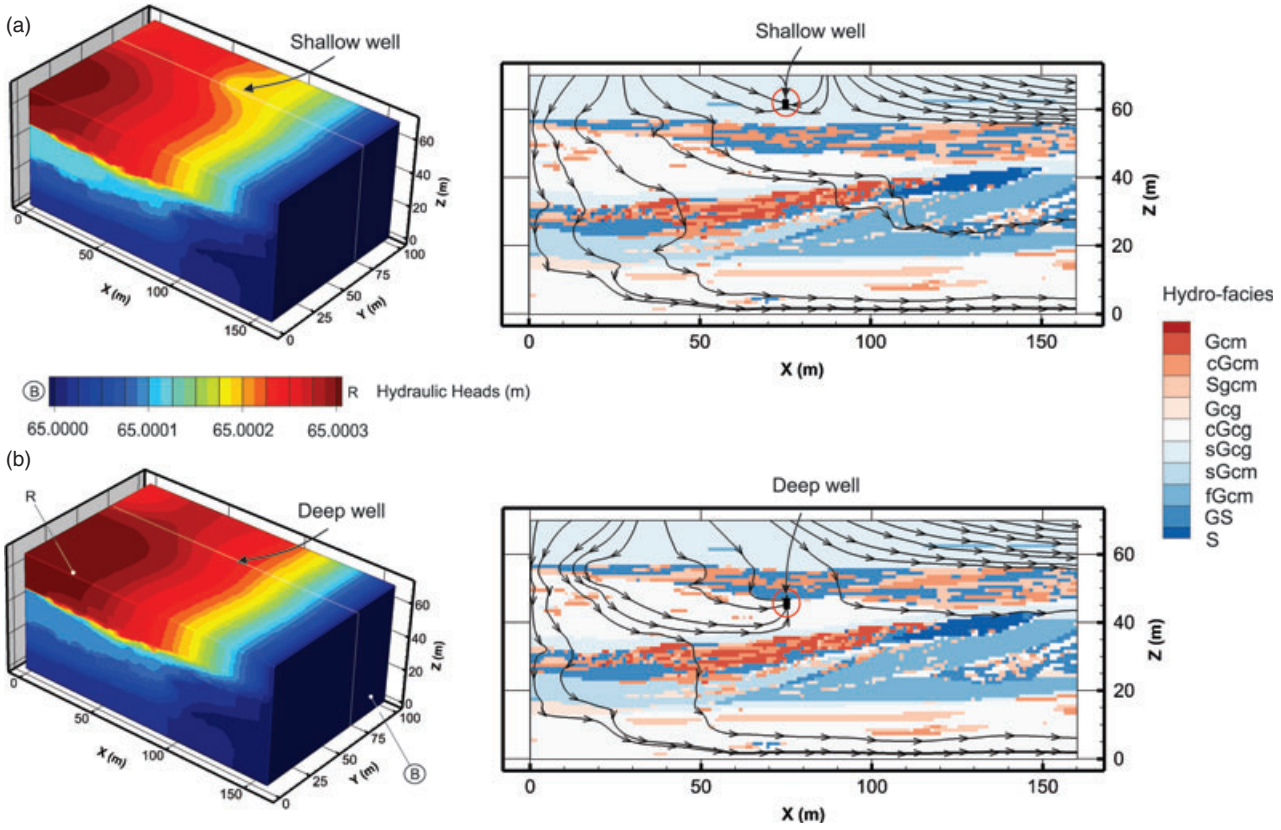

Figure 3. (a) Simulated steady-state hydraulic heads (m) with a shallow pumping/observation well for the Herten aquifer (left) and cross section at $y = 75$ m showing groundwater tangent flow lines and hydro-facies (right). (b) Simulated steady-state hydraulic heads (m) with a deep pumping/observation well and cross section at $y = 75$ m showing groundwater flow lines and hydro-facies. B with the circle means Blue (for black and white printing).

Table 2
DPSIR Analysis for Groundwater Source Vulnerability (Scenario 1) and Groundwater Resource Vulnerability (Scenarios 2 and 3)

	P	UF	ST	DF	I
Scenario 1	Climate change	Groundwater recharge	—	Hydraulic head at a well	Groundwater depletion (quantity)
Scenario 2	Groundwater demand	Groundwater intake	Groundwater quantity	—	Groundwater depletion (quantity)
Scenario 3	Climate change	Groundwater recharge	Groundwater quantity	—	Groundwater depletion (quantity)

P, pressure; UF, upstream factor; ST, state; DF, downstream factor; I, impact.

aquifer (Figure 5). Therefore, an efficient hydraulic link causes the head in the deep observation well to respond strongly to small changes in groundwater recharge rates where sensitivity coefficient is now larger. These hydraulic links exist because of the complex structure of the aquifer, which makes intuitive predictions difficult.

Although this scenario is rather simple because it only considers steady-state fully-saturated flow, we could think that the performance measure should be located where any change in hydraulic head might be critical, for example, close to rivers, wetlands, or pumping wells. The sensitivity map would then be useful for land use planning and groundwater protection as planners could try to protect first the surface areas where the recharge is important to maintain groundwater levels at the observation well location. This also shows that the performance measure is an arbitrary choice made by land-use planners and is likely case-dependent. Different simulations have to be conducted for every scenario envisioned by the planners. Each scenario should depend on pressures and user-defined parameters, while the different simulations should be based on different targeted areas and performance measures.

The sensitivity coefficients could be converted to vulnerability coefficients using Equation 6. To compute the vulnerability coefficients, we assume that the hydraulic

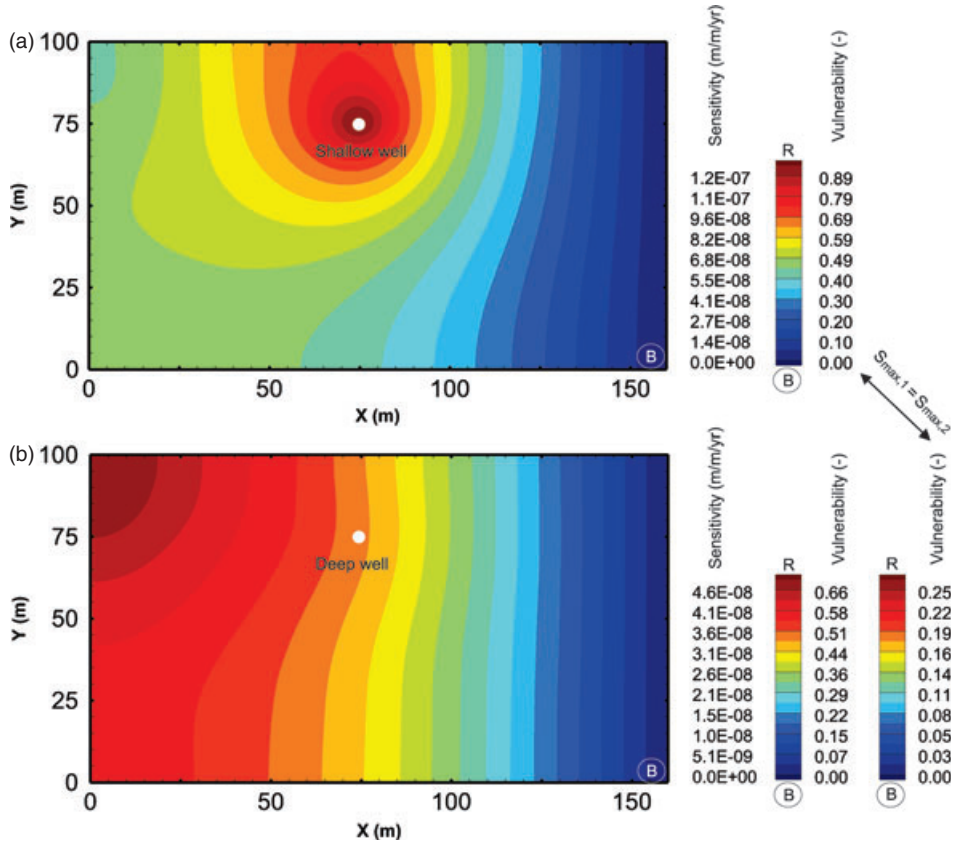

Figure 4. Simulated source sensitivity coefficients and source vulnerability coefficients for (a) the groundwater head in the shallow pumping/observation well and (b) the groundwater head in the deep pumping/observation well (surficial plane view). The rightmost legend refers to the values normalized with a common maximum sensitivity coefficient.

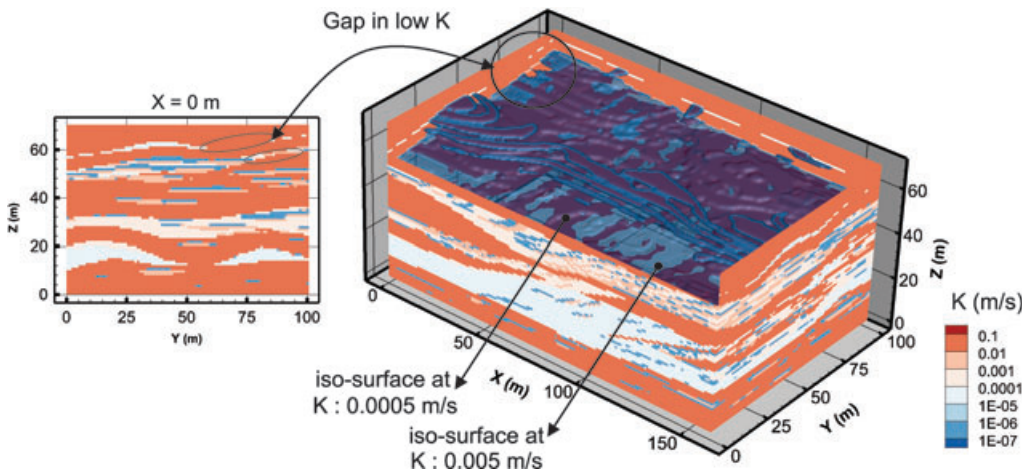

Figure 5. Hydraulic conductivity distribution at $x = 0$ m. The pinching and thinning of the two upper low-K layers are responsible for the distribution of the sensitivity coefficients as shown in Figure 4b.

head at the location of the performance measure should not be lower than a threshold value of 45 m for Model 1 (i.e., $W_0 = 45$ m; Figure 4a) and 61 m for Model 2 (i.e., $W_0 = 61$ m; Figure 4b). Thus in both models, 1 m head in each well is assumed to be sufficient to sustain groundwater pumping/utilization and to avoid drying up of the wells. The vulnerability maps are similar to the sensitivity maps because the ratio in Equation 5 is a constant, but the values are different. On the one hand, they are relative to their respective maximum sensitivity coefficient and embody a distance to a threshold. Choosing another value W_0 for the threshold would yield different vulnerability values. On the other hand, the sensitivity coefficients are independent of this choice. The advantage of using the vulnerability maps rather than the sensitivity maps is for decision making. For example, water levels

can be very sensitive to recharge rates in some parts of an aquifer, but their vulnerability can be low if their distance to the threshold is large. Surprisingly, the vulnerability can still be low if the current state is close to the threshold. However, the sensitivity can be so low with respect to the maximum sensitivity coefficient that the current damaged state is not getting worse. In a decisional scheme, end-users may also wonder about comparison between the two models when examining vulnerability or the ability of possible responses to reduce the vulnerability. Consequently, vulnerability coefficients could be normalized with a common maximum sensitivity coefficient as in Equation 6 (Figure 4).

Resource Vulnerability

In the second example, the GRV is assessed using the sensitivity equation method. Here, two other scenarios are considered (Table 2). In Scenario 2, overexploitation is the pressure and the ST is the change in groundwater quantity. Groundwater depletion is the impact. In this

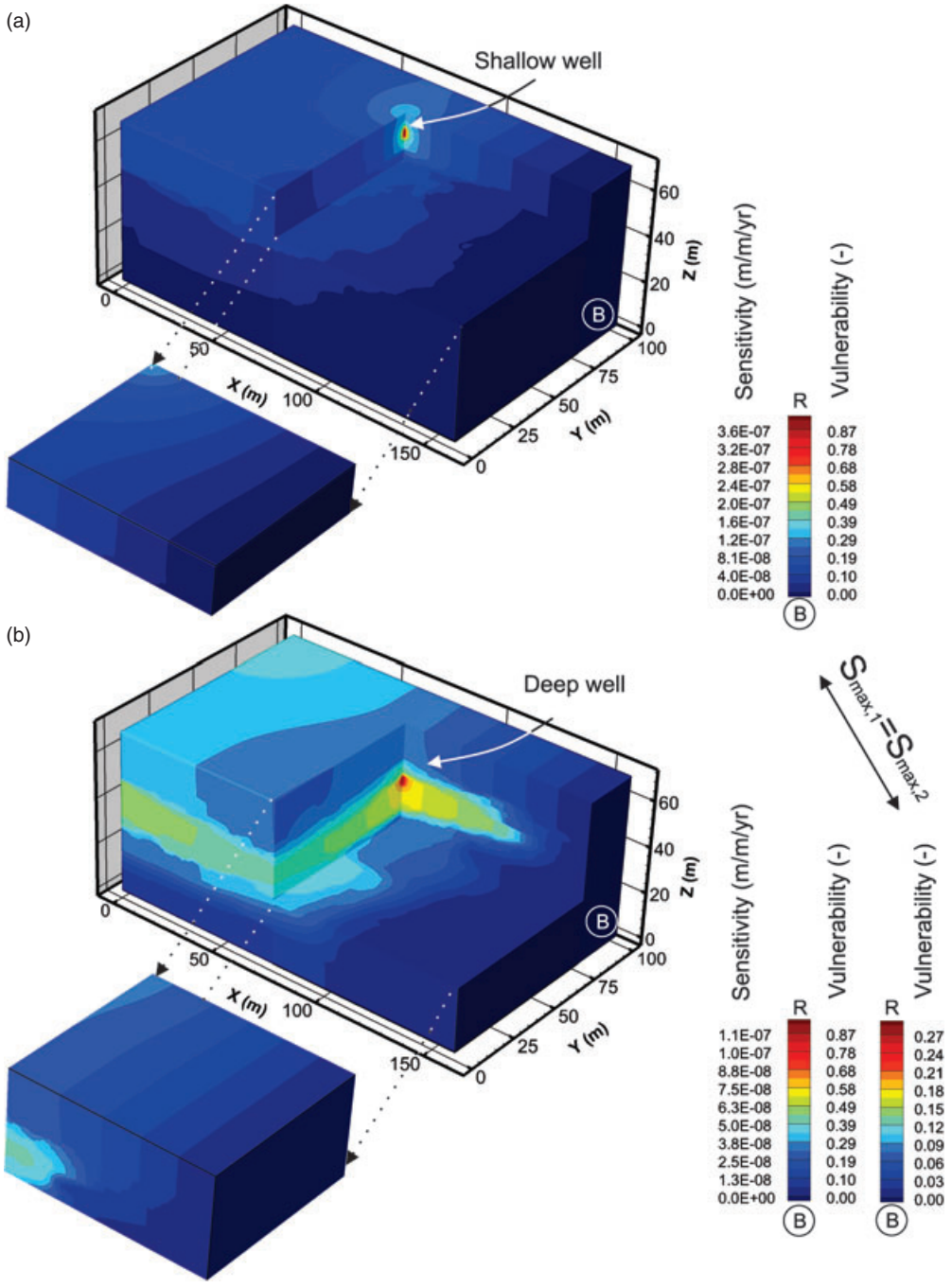

Figure 6. Simulated resource sensitivity coefficients and resource vulnerability coefficients for the groundwater heads in the aquifer with respect to an elemental change in groundwater abstraction in (a) a shallow pumping/observation well and (b) a deep pumping/observation well. The rightmost legend refers to values normalized with a common maximum sensitivity coefficient.

scenario, both Models 1 and 2 are addressed. In each model, the sensitivity of all hydraulic heads is evaluated with respect to a change in the well discharge rate. The shallow and deep wells are still tapping the sGcg and cGcg hydro-facies, respectively. Figure 6a and 6b illustrates the portions of the aquifer that are the most sensitive to a change in the well discharge rate. The distribution of sensitivity coefficients is similar to the distribution of hydraulic heads (Figure 3a and 3b). However, hydraulic heads are more sensitive in Model 1 than in Model 2 because the deep well is tapping a semi-confined high hydraulic conductivity facies. This leads to smoothing of the aquifer response in terms of hydraulic head and thus sensitivity coefficient.

In Scenario 3, climate change is the pressure and the ST is the change in groundwater quantity. Here, Model 1 is addressed. However, the sensitivity of all hydraulic heads within the model is evaluated with respect to a change in overall groundwater recharge. Groundwater depletion is the impact. Figure 7 shows that the distribution of sensitivity coefficients is close, but not identical, to the distribution of hydraulic heads. This result is predictable because an increase in overall recharge will result in an overall increase in hydraulic heads. The upper part of the aquifer is most sensitive to a change in recharge rates. The lower part of the aquifer is rather insensitive because of the presence of a low hydraulic conductivity facies located at about half-depth within the aquifer. Moreover, the sensitivity is minimum close to the specified head boundary because the heads remain unchanged.

The resource sensitivity provides substantial information to the understanding of the groundwater flow system. In Scenario 2, it helps planners to setup pumping wells or to protect the most sensitive area (e.g., with artificial recharge). In Scenario 3, it shows what portions of the aquifer are the most sensitive to an overall change in groundwater recharge. Here, we have used a single uniform recharge at the ground surface, but we could perform the calculations with different zones having different groundwater recharge rates. In this case, we would get a number of different sensitivity maps equal to the number of recharge zones at the surface.

GRV could also be evaluated using a threshold. Here, a spatially distributed hydraulic head of 60 m is assumed to be the threshold. In Scenario 3, this threshold cannot be reached by the current degradation state, even if the recharge rate on the top of the model is set to zero. However, the downstream boundary condition that mainly controls the groundwater level may change over time as a consequence, for example, of climate change. This makes a hydraulic head of 60 m a realistic and easily accessible threshold value if the hydraulic head drop by a few meters. The vulnerability contours are given in Figure 6 for Scenario 2, and in Figure 7 for Scenario 3. As for the source vulnerability, the contours are similar to the sensitivity contours, except that the values are different and depend on the selected threshold. Here, the ratio in Equation 5 is not constant anymore but varies slightly spatially. Indeed, the ratio remains close to 1 because of a weak horizontal gradient in the upper layer and a small range of hydraulic head values. The results also show that

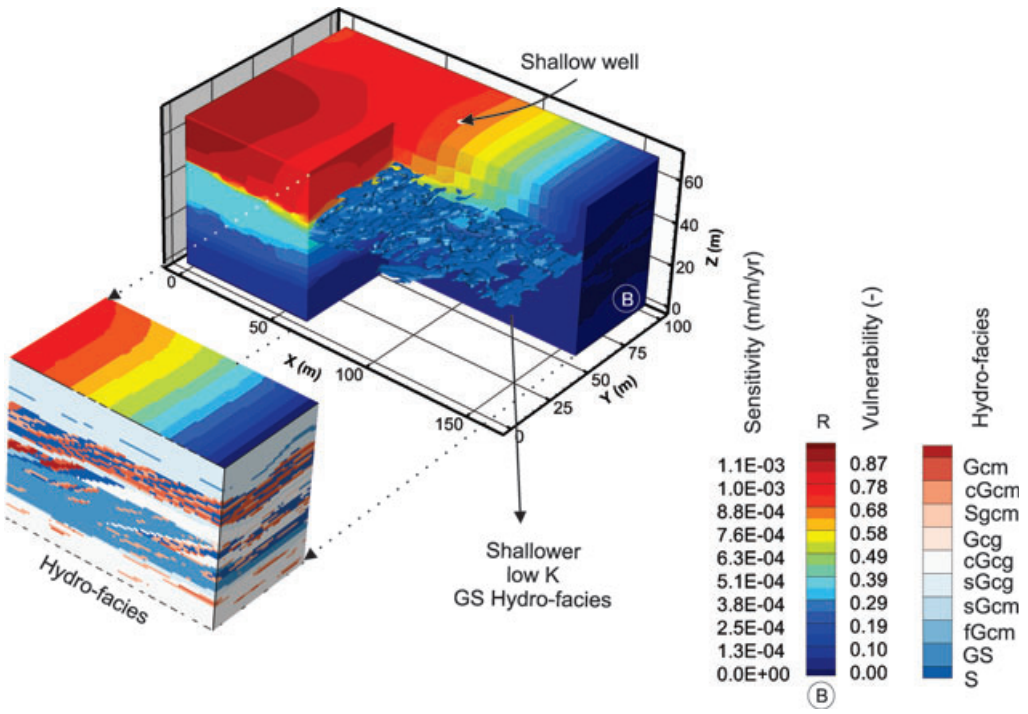

Figure 7. Simulated resource sensitivity coefficients and resource vulnerability coefficients for the groundwater heads in the aquifer with respect to an elemental change in groundwater recharge. A low hydraulic conductivity facies makes the upper part of the aquifer the most sensitive.

the current degradation state is not unique owing to the pressure identified in the DPSIR analysis. In particular, in Scenario 3 where the recharge is the pressure of concern, the presence of another already existing external pressure (i.e., the shallow pumping well) is not of importance because what is of interest for the planners is the change in vulnerability coefficient due to a significant change in the selected pressure (i.e., overall recharge) or a chosen alternative response, all other parameters being equal.

In this example, the groundwater resource sensitivity and vulnerability are displayed as a set of 3D contours, which are not useful to use in GIS and are more difficult to understand by nonspecialists. However, contours for a specific depth could be extracted (e.g., water table elevation or contours within a specific aquifer), in order to display the results on 2D maps.

Computational Effort

The sensitivity coefficients for the GSV were computed using the adjoint operator method because we have demonstrated that it is the most efficient. It required only two steady-state simulations compared to 16,001 simulations for a differential approach, which is equal to the number of nodes at the surface of the model plus one. On the other hand, the GRV was computed using the sensitivity equation method and required only two steady-state simulations. It would have required 1,120,001 simulations with the adjoint equation method, which is the number of nodes in the model plus one. This clearly demonstrates the importance of choosing the right method for computing the sensitivity coefficients.

Conclusion

This paper presents a new physically based groundwater vulnerability assessment methodology that relies on sensitivity analysis methods. The sensitivity equation and the adjoint operator methods are considered. We show how the careful selection of a method can minimize the computational effort. We show that the sensitivity equation method is more efficient to assess GRV, whereas the adjoint operator method is most efficient for GSV assessment.

The methodology also relies on the definition of causal chains that relate pressure, groundwater state, and impacts. While the methodology is general, the choice of causal chains has to be made prior to the calculation. The vulnerability is also related to a damaged state and is related to the distance between the current state and a threshold. This choice is arbitrary such that the vulnerability is sensitive to the choice of the threshold. On the other hand, the sensitivity coefficients are insensitive to this choice and can be used as a proxy for the vulnerability of the resource.

The methodology was demonstrated with the Herten aquifer analog, which is a complex glacio-fluvial aquifer, to assess the GSV and GRV to changes in recharge rates at the ground surface and the GRV to changes in well discharge rates. The results highlight that, in complex aquifers, the source vulnerability is not readily predictable and that numerical models are useful for their prediction. The results also suggest that the resource vulnerability maps do not necessarily match the sensitivity contours. In others applications, this may be encountered when the sensitivity map does not match perfectly the hydraulic heads distribution. In addition, a wider range of hydraulic heads is expected to show that the resource vulnerability is not readily predictable either. Finally, the demonstration highlights the usefulness of the method for land-use planning and for protecting portions of the aquifer that are more sensitive to pressures. For example, planners may test the efficiency of alternative responses, the efficiency being expressed in terms of vulnerability reduction, and take advantage of it for decision making. The methods yield a set of maps that could be used in GIS and understood by nonspecialists.

While the theory outlined in this paper is restricted to groundwater flow, it could be extended to solute transport as well as groundwater age. It is also flexible as many different performance measures, state variables, and pressures can be defined. It is also amenable to multicriteria decision analysis methods. Finally, the method can also be used at multiple scales (local to regional).

However, application of the adjoint method is not straight forward for nonlinear equations such as that for unsaturated flow. The adjoint operator is only formally defined for linear operators. Furthermore, the transport equation is not self-adjoint (unlike flow), which means that the transport adjoint equation is not identical to the forward equation. Finally, in transient problems, the adjoint method requires a cumbersome marching forward in time and then reverse time stepping.

The method also relies on availability of a well-calibrated model, which is not always the case, especially for complex aquifers. The sensitivity equation method as well as the adjoint operator methods also require minor code modifications.

Acknowledgments

This work was supported by the European Union FP6 STREP Project number 518118-1 GABARDINE under the thematic priority Sustainable Development, Global Change and Ecosystems. The University of Liège is acknowledged for the financial support of J.-M.L. through a postdoctoral fellowship. Pierre Therrien of Université Laval is greatly acknowledged for simulation support and Nicolas Gardin for initial works on the theoretical concepts.

Supporting Information

Additional Supporting Information may be found in the online version of this article:

Appendix S1. A description of the different numerical methods used to compute the sensitivity coefficients.

References

Ahlfeld, D.P., J.M. Mulvey, G.F. Pinder, and E.F. Wood. 1988. Contaminated groundwater remediation design using simulation, optimization, and sensitivity theory 1. Model development. *Water Resources Research* 24, no. 3: 431–441.

Aller, L., T. Bennet, H.J. Lehr, J.R. Petty, and G. Hackett. 1987. DRASTIC a standardized system for evaluating ground water pollution potential using hydrogeologic settings. Technical Report EPA-600/2-87-035. US EPA.

Bayer, P., P. Huggenberger, P. Renard, and A. Comunian. 2011. Three-dimensional high resolution fluvio-glacial aquifer analog, Part 1: Field study. *Journal of Hydrology* 405, no. 1–2: 1–9.

Beaujean, J., P. Wojda, N. Gardin, and S. Brouyère. 2008. DL44 methodology and setup of the adopted groundwater vulnerability assessment method. Technical Report 518118-1, University of Liège, Hydrogeology and Environmental Geology and Aquapôle, Liège, Belgium. http://hdl.handle.net/2268/77251 (accessed April 15, 2011).

Brouyère, S., P.Y. Jeannin, A. Dassargues, N. Goldscheider, I.C. Popescu, M. Sauter, I. Vadillo, and F. Zwahlen. 2001. Evaluation and validation of vulnerability concepts using a physically based approach. In *Proceedings of the 7th Conference on Limestone Hydrology and Fissured Media, Sciences et Techniques de l' Environnement. Mémoire hors-série*, 67–72. Besançon: Université de Franche-Comté.

Comunian, A., P. Renard, J. Straubhaar, and P. Bayer. 2011. Three-dimensional high resolution fluvio-glacial aquifer analog, Part 2: Geostatistical modelling. *Journal of Hydrology* 405, no. 1–2: 10–23.

Doerfliger, N., P.Y. Jeannin, and F. Zwahlen. 1999. Water vulnerability assessment in karst environments a new method of defining protection areas using a multi-attribute approach and GIS tools (EPIK method). *Environmental Geology* 39, no. 2: 165–176.

EEA. 2003. Environmental indicators: Typology and use in reporting. EEA Internal Working Paper EPA-600/2-87-035, EEA Internal Working Paper.

Foster, S.S.D. 1987. Fundamental concepts in aquifer vulnerability, pollution risk and protection strategy. In *Vulnerability of Soil and Groundwater to Pollutants*, ed. W. van Duijvenbooden and H.G. van Waegeningh, 69–86. Gravenhage, The Netherlands: Committee for Hydrological Research T.N.O.

Frind, E.O., J.W. Molson, and D.L. Rudolph. 2006. Well vulnerability: A quantitative approach for source water protection. *Ground Water* 44, no. 5: 732–742. DOI:10.1111/j.1745-6584.2006.00230.x.

Gardin, N., P. Wojda, and S. Brouyere. 2006. Dl43 stress factors and associated physically-based criteria and conclusions on the directions to be followed for developing a physically-based vulnerability assessment method. Technical Report 518118-1, University of Liège, Hydrogeology and Environmental Geology and Aquapôle, Liège, Belgium. http://hdl.handle.net/2268/153189 (accessed May 27, 2011).

Gogu, R.C., V. Hallet, and A. Dassargues. 2003. Comparison of aquifer vulnerability assessment techniques. Application to the Néblon river basin (Belgium). *Environmental Geology* 44, no. 8: 881–892. DOI:10.1007/s00254-003-0842-x.

Gogu, R.C., and A. Dassargues. 2000. Current and future trends in groundwater vulnerability assessment. *Environmental Geology* 39, no. 6: 549–559. DOI:10.1007/s002540050466.

Jyrkama, M.I., and J.F. Sykes. 2006. Sensitivity and uncertainty analysis of the recharge boundary condition. *Water Resources Research* 42, no. 1: W01404. DOI:10.1029/2005JD004408.

Kristensen, P. 2004. The DPSIR framework. workshop on a comprehensive/detailed assessment of the vulnerability of water resources to environmental change in Africa using river basin approach, 27–29 September, Nairobi, Kenya, UNEP Headquarters.

Luers, A.L., D.B. Lobel, L.S. Sklar, C.L. Addams, and P.A. Matson. 2003. A method for quantifying vulnerability, applied to the agricultural system of the Yaqui Valley, Mexico. *Global Environmental Change* 13, no. 4: 255–267.

Molson, J.W., and E.O. Frind. 2012. On the use of mean groundwater age, life expectancy and capture probability for defining aquifer vulnerability and time-of-travel zones for source water protection. *The Journal of Contaminant Hydrology* 127, no. 1–4: 76–87. DOI:10.1016/j.jconhyd.2011.06.001.

Neukum, C., H. Hoetzl, and T. Himmelsbach. 2008. Validation of vulnerability mapping methods by field investigations and numerical modelling. *Hydrogeology Journal* 16, no. 4: 641–658. DOI:10.1007/s10040-007-0249-y.

Popescu, I.C., N. Gardin, S. Brouyère, and A. Dassargues. 2008. Groundwater vulnerability assessment using physically based modelling: from challenges to pragmatic solutions. In *Calibration and Reliability in Groundwater Modelling*, ed. J.C. Refsgaard, K. Kovar, E. Haarder, and E. Nygaard, 83–88 (ModelCARE'07, Copenhagen, Denmark, September 2007). Wallingford, UK: IAHS Press.

Sun, N.-Z., and W.W.-G. Yeh. 1990. Coupled inverse problems in groundwater modeling 1. Sensitivity analysis and parameter identification. *Water Resources Research* 26, no. 10: 2507–2525.

Sykes, J.F., J.L. Wilson, and R.W. Andrews. 1985. Sensitivity analysis for steady state groundwater flow using adjoint operators. *Water Resources Research* 21, no. 3: 359–371.

Therrien, R., R. McLaren, E.A. Sudicky, and S. Panday. 2006. *HydroGeoSphere, A Three-dimensional Numerical Model Describing Fully-Integrated Subsurface and Surface Flow and Solute Transport*. Waterloo, Canada: Groundwater Simulations Group, University of Waterloo. Groundwater Simulations Group.